Spectral-Domain Analysis of Open and Shielded Slotlines Printed on Various Anisotropic Substrates

Yinchao Chen and Benjamin Beker, *Member IEEE*

Abstract—**A rigorous full-wave analysis based on the spectral-domain approach for open and shielded slotline transmission lines is presented. The substrate materials under consideration are anisotropic, characterized by both their permittivity and permeability tensors. The formulation includes off-diagonal tensor elements to represent gyroelectric media, Ferrites, or the misalignment between the principal axes of the substrate and the coordinate system of the waveguide. Dyadic admittance Green's functions for every structure are obtained with the help of differential matrix operators in the Fourier-transformed domain, and the Galerkin method is employed to find the propagation constants numerically.**

I. Introduction

THE SHIELDED slotline (or finline) has been used at microwave and millimeter-wave frequencies for quite some time [1]. Its analog, the open slotline, has enjoyed wide popularity in various applications at these frequencies as well [2]. Desirable features of shielded slotlines include reduced size, weight, and ease of integration into the overall microwave integrated circuit (MIC). Advantages of open slotlines, which are often used in microstrip antenna feeding networks [3], include reduction in the radiation level back to the feeding circuit.

The majority of past and present work has focused on slotlines with isotropic substrates only (see [1], [2], and [4]–[6]). More recently however, anisotropic substrates have been considered as well, including shielded finlines [7], [8], partially covered slotlines [9], as well as fully open structures [10], [11]. Although the cited references laid out the ground work for such structures, none of them considered bilateral open slotlines printed on general anisotropic media in detail.

This paper presents the spectral-domain formulation and numerical results for the dispersive characteristics of open as well as shielded slotline transmission lines. The odd and even modes of open bilateral slotlines are examined. The former corresponds to the electric wall bisecting the plane of symmetry, whereas the later considers the magnetic wall case. In addition, an analysis of shielded bilateral slotlines (finlines) is also included to illustrate the similarities in their propagation characteristics compared to those of open structures.

Manuscript received May 14, 1992; revised January 19, 1993.

The authors are with the Department of Electrical and Computer Engineering, University of South Carolina, Columbia, SC, 29208.

IEEE Log Number 9210213.

It is known that open slotlines leak power into the dielectric-filled parallel plate waveguide (PPW) regions. For electric (PEC) conductor-backed structures, the leakage is always present, but is small if appropriate values of medium parameters and geometrical dimensions are employed [5]. The same is also true for a magnetic (PMC) conductor-backed slotline, with the only difference being that the modes of this parallel-plate structure have a cuff-off frequency [4]. In this paper, all physical dimensions and medium parameters are chosen so as to minimize the leakage effects, since the paper aims at emphasizing the influence of substrate anisotropy on the propagation characteristics of bilateral slotlines.

In what follows, it is assumed that every MIC transmission line is printed on a homogeneous anisotropic substrate that has its optical axes of the permittivity and permeability arbitrarily oriented in the xz-plane, i.e., the plane of propagation. As a result, the theory presented in this work encompasses a wide variety of guiding media, which can be either gyroelectric, Ferrite, or both. When off-diagonal tensor elements of $[\varepsilon]$ and $[\mu]$ are real, the tensors are symmetric, then misalignment between coordinates of the waveguide and those of the material tensors can be examined well.

Dyadic admittance Green's functions for every transmission line are formulated using differential matrix operators [12], and the spectral-domain approach [13, Chapter 5]. The propagation constants of dominant modes are obtained by using the Galerkin method. Both electric and magnetic wall symmetries (odd and even modes, respectively) for open structures and the magnetic wall symmetry for shielded bilateral slotlines are considered. The basis functions used to expand the field inside the slot are carefully chosen with build-in edge singularities. The formulation and the numerical approach are validated against the available published data from references [4], [6], and [7].

II. Admittance Green's Functions For Anisotropic Substrates

Crossectional view of waveguides that are under consideration in this paper are shown in Fig. 1. The substrate material is assumed to be characterized by the permittivity tensor which can be either gyroelectric (Hermitian) or misaligned with the coordinates of the structure in the xz-plane. For generality, the constitutive properties of the substrate also include the anisotropic nature of the permeability tensor, which can represent a Ferrite or the rotation effects of its principal

(material) axes. All the aforementioned medium characteristics can be incorporated into the formulation by the following tensor forms:

$$\varepsilon_0[\varepsilon_r] = \varepsilon_0 \begin{bmatrix} \varepsilon_{xx} & 0 & \varepsilon_{xz} \\ 0 & \varepsilon_{yy} & 0 \\ \varepsilon_{zx} & 0 & \varepsilon_{zz} \end{bmatrix} \tag{1a}$$

and

$$\mu_0[\mu_r] = \mu_0 \begin{bmatrix} \mu_{xx} & 0 & \mu_{xz} \\ 0 & \mu_{yy} & 0 \\ \mu_{zx} & 0 & \mu_{zz} \end{bmatrix}, \tag{1b}$$

where

$$\varepsilon_{xx} = \varepsilon_{x1}\cos^2\theta + \varepsilon_{z1}\sin^2\theta \tag{2a}$$
$$\varepsilon_{yy} = \varepsilon_{y1} \tag{2b}$$
$$\varepsilon_{xz} = \varepsilon_{zx} = (\varepsilon_{z1} - \varepsilon_{x1})\sin\theta\cos\theta \tag{2c}$$
$$\varepsilon_{zz} = \varepsilon_{x1}\sin^2\theta + \varepsilon_{z1}\cos^2\theta \tag{2d}$$

$$\mu_{xx} = \begin{cases} 1 - \dfrac{\mu_0^2\gamma_0^2 M_s H_0}{\omega^2 - (\mu_0\gamma_0 H_0)^2} \\ \text{or} \\ \mu_{x2}\cos^2(\theta + \Delta\theta) + \mu_{z2}\sin^2(\theta + \Delta\theta) \end{cases} \tag{3a}$$

$$\mu_{yy} = \begin{cases} 1 \\ \text{or} \\ \mu_{y2} \end{cases} \tag{3b}$$

$$\mu_{xz} = \begin{cases} -\mu_{zx} = jk_r = \dfrac{-j\,\mu_0\gamma_0 M_s\omega}{\omega^2 - (\mu_0\gamma_0 H_0)^2} \\ \text{or} \\ \mu_{zx} = (\mu_{z2} - \mu_{x2})\sin(\theta + \Delta\theta)\cos(\theta + \Delta\theta) \end{cases} \tag{3c}$$

$$\mu_{zz} = \begin{cases} 1 - \dfrac{\mu_0^2\gamma_0^2 M_s H_0}{\omega^2 - (\mu_0\gamma_0 H_0)^2} \\ \text{or} \\ \mu_{x2}\sin^2(\theta + \Delta\theta) + \mu_{z2}\cos^2(\theta + \Delta\theta) \end{cases} \tag{3d}$$

In the above equations, θ and $\Delta\theta$ refer to the misalignment angles between the coordinates of the line and principal axes of $[\varepsilon]$ and $[\mu]$; namely, between the (x, y, x) and (x_1, y_1, z_1) or (x_2, y_2, z_2) coordinates. The quantities $(\varepsilon_{x1}, \varepsilon_{y1}, \varepsilon_{z1})$ and $(\mu_{x2}, \mu_{y2}, \mu_{z2})$ are the principal values of the diagonalized permittivity and permeability tensors in these coordinate systems. The operating angular frequency is ω, with H_0, M_s, and γ_0 corresponding to the magnitude of the applied dc magnetic field, magnetization, and the gyromagnetic ratio, respectively [14].

The derivation of the Green's function begins with the two Maxwell's curl relations that inside the anisotropic region, following Fourier transformation, have the following forms [12]:

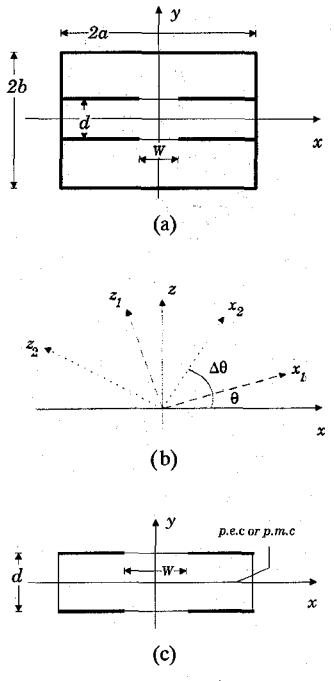

Fig. 1. Problem geometry. (a) Shielded bilateral slotline (finline). (b) Waveguide and medium tensor coordinates. (c) Open bilateral slotline.

$$\begin{bmatrix} 0 & j\beta & \frac{d}{dy} \\ -j\beta & 0 & j\alpha \\ -\frac{d}{dy} & -j\alpha & 0 \end{bmatrix} \begin{bmatrix} \begin{pmatrix} \tilde{E}_x \\ \tilde{H}_x \end{pmatrix} \\ \begin{pmatrix} \tilde{E}_y \\ \tilde{H}_y \end{pmatrix} \\ \begin{pmatrix} \tilde{E}_z \\ \tilde{H}_z \end{pmatrix} \end{bmatrix} = j\omega \begin{pmatrix} -\mu_0 \\ \varepsilon_0 \end{pmatrix} \begin{bmatrix} \begin{pmatrix} \mu_{xx} \\ \varepsilon_{xx} \end{pmatrix} & 0 & \begin{pmatrix} \mu_{xz} \\ \varepsilon_{xz} \end{pmatrix} \\ 0 & \begin{pmatrix} \mu_{yy} \\ \varepsilon_{yy} \end{pmatrix} & 0 \\ \begin{pmatrix} \mu_{zx} \\ \varepsilon_{zx} \end{pmatrix} & 0 & \begin{pmatrix} \mu_{zz} \\ \varepsilon_{zz} \end{pmatrix} \end{bmatrix} \begin{bmatrix} \begin{pmatrix} \tilde{H}_x \\ \tilde{E}_x \end{pmatrix} \\ \begin{pmatrix} \tilde{H}_y \\ \tilde{E}_y \end{pmatrix} \\ \begin{pmatrix} \tilde{H}_z \\ \tilde{E}_z \end{pmatrix} \end{bmatrix}, \tag{4a,b}$$

where α is the transform variable and β is the propagation constant in the positive z-direction. The use of (4a) in (4b) allows for elimination of the H-field using simple matrix algebra rather than tedious manipulation of individual field components. This procedure leads to a matrix equation for the three components of electric field

$$\begin{bmatrix} a_{11} & a_{12} & a_{13} \\ a_{21} & a_{22} & a_{23} \\ a_{31} & a_{32} & a_{33} \end{bmatrix} \begin{bmatrix} \tilde{E}_x \\ \tilde{E}_y \\ \tilde{E}_z \end{bmatrix} = \begin{bmatrix} 0 \\ 0 \\ 0 \end{bmatrix} \tag{5}$$

where $a_{ij}s(i, j = 1, 2, 3)$ appearing in (5) are linear differential operators given in the Appendix.

Further simplifications to (5), namely elimination of $\tilde{E}_y$ (the normal component of $\vec{\tilde{E}}$ to the air-substrate interface), result in two equations containing the desired pair of the tangential E-field components, $\tilde{E}_x$ and $\tilde{E}_z$. These components are still coupled to one another, as is shown below:

$$\begin{bmatrix} a_2\frac{d^2}{dy^2} + a_0 & b_2\frac{d^2}{dy^2} + b_0 \\ c_2\frac{d^2}{dy^2} + c_0 & d_2\frac{d^2}{dy^2} + d_0 \end{bmatrix} \begin{bmatrix} \tilde{E}_x \\ \tilde{E}_z \end{bmatrix} = \begin{bmatrix} 0 \\ 0 \end{bmatrix} \tag{6}$$

where constant coefficients a_0 through d_2 are also defined in the Appendix.

Nontrivial solutions to (6) for the transverse propagation parameter γ, require for the determinant of (6) to vanish. Assuming that both tangential components of $\tilde{E}$ must have the same functional variation along the y-direction, namely, $e^{\gamma y}$, leads to the following equation for γ:

$$(a_2\gamma^2 + a_0)(d_2\gamma^2 + d_0) - (b_2\gamma^2 + b_0)(c_2\gamma^2 + c_0) = 0. \tag{7}$$

The roots of the above equation will give the general solutions for $\tilde{E}_x$ and $\tilde{E}_z$ in the anisotropic region in terms of hyperbolic sine and cosine functions. However, the specific solutions for $\tilde{E}_x$ and $\tilde{E}_z$ depend on boundary conditions at the $y = 0$ plane, which is the symmetry wall of the structure. Since this wall can be either a perfect magnetic or electrical conductor, the two sets of possible solutions are

$$\tilde{E}_x(\alpha, y) = -A_1\left(\frac{b_2\gamma_a^2 + b_0}{a_2\gamma_a^2 + a_0}\right)\begin{Bmatrix}\cos h\gamma_a y\\ \sin h\gamma_a y\end{Bmatrix} - A_2\left(\frac{b_2\gamma_b^2 + b_0}{a_2\gamma_b^2 + a_0}\right)\begin{Bmatrix}\cos h\gamma_b y\\ \sin h\gamma_b y\end{Bmatrix} \tag{8a}$$

$$\tilde{E}_z(\alpha, y) = A_1\begin{Bmatrix}\cos h\gamma_a y\\ \sin h\gamma_a y\end{Bmatrix} + A_2\begin{Bmatrix}\cos h\gamma_b y\\ \sin h\gamma_b y\end{Bmatrix} \tag{8b}$$

where the upper set corresponds to the magnetic wall, lower set refers to the electric wall, and parameters γ_a and γ_b are roots of (7). Finally, all remaining field components can now be expressed in terms $\tilde{E}_x$ and $\tilde{E}_z$ by using Maxwell's curl equations.

The field inside the isotropic region can be found by using scalar electric and magnetic potentials [13, p. 337]. Once the field expressions in every region are known, then their tangential components can be matched at the air-substrate boundary, the procedure that leads to the dyadic admittance Green's function

$$\begin{bmatrix}\tilde{Y}_{zz}(\alpha,\beta) & \tilde{Y}_{zx}(\alpha,\beta)\\ \tilde{Y}_{xz}(\alpha,\beta) & \tilde{Y}_{xx}(\alpha,\beta)\end{bmatrix}\begin{bmatrix}\tilde{E}_z(\alpha)\\ \tilde{E}_x(\alpha)\end{bmatrix} = \begin{bmatrix}\tilde{J}_z(\alpha)\\ \tilde{J}_x(\alpha)\end{bmatrix} \tag{9}$$

whose elements appear in the Appendix.

Finally, to obtain the propagation constants, β, the electric fields in the slot are expanded in terms of a weighted sum of the following basis functions:

$$\tilde{E}_{xn}(x) = \frac{\cos\left[(n-1)\pi\frac{x}{W/2}\right]}{\sqrt{(W/2)^2 - x^2}} \qquad n = 1, 2, 3, \cdots, \tag{10a}$$

$$\tilde{E}_{zm}(x) = \frac{\sin\left[m\pi\frac{x}{W/2}\right]}{\sqrt{(W/2)^2 - x^2}} \qquad m = 1, 2, 3, \cdots, \tag{10b}$$

where W is the width of the slot. When the Fourier transforms of (10a) and (10b) are substituted back into (9), and appropriate inner products are taken, a system of matrix equations is obtained whose determinant can be used to find the propagation constants.

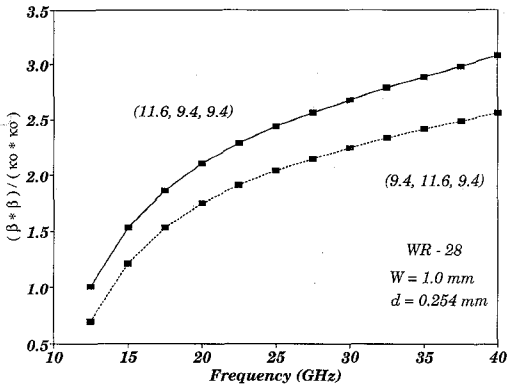

Fig. 2. Frequency dependence of ε_{eff} for a shielded bilateral finline on sapphire substrate: (— and ----- this method, ■■■ data from [7]).

TABLE I
COMPARISON OF CALCULATED OPEN ELECTRIC CONDUCTOR-BACKED SLOTLINE DATA

$f(\text{GH}_z)$	10	20	30	40	50
ε_{eff}	6.878	6.880	6.882	6.8834	6.9026
ε_{eff} [6]	6.922	6.935	6.951	6.9700	6.9950

TABLE II
COMPARISON OF CALCULATED OPEN MAGNETIC CONDUCTOR-BACKED SLOTLINE DATA

$\sqrt{\varepsilon_r - 1}\,(\frac{d}{\lambda_0})$	0.0458	0.0687	0.0917	0.1146	0.1375
ε_{eff}	5.452	5.990	6.317	6.5614	6.5880
ε_{eff} [4]	5.723	6.002	6.319	6.5618	6.6443

III. NUMERICAL RESULTS

To validate the theory and the numerical results, three structures were considered. Tables I and II provide a comparison summary for open, electric, and magnetic conductor-backed slotlines. The agreement between the computed and previously published data for Gallium Arsenide ($\varepsilon_r = 12.9$) substrate is seen to be quite good. Notice that the results in Tables I and II, obtained from [6] and [4], when compared to those computed using the theory presented herein are slightly different. This, however, can be attributed to the magnetic rather than open side walls used in the respective formulations. In addition, Fig. 2 also displays results of validation studies for the shielded bilateral finline that is printed on sapphire [7]. As can be seen, the agreement between the two sets of data for the enclosed structure is also very good.

Next, Figs. 3 and 4 illustrate the properties of the open conductor-backed slotlines printed on anisotropic substrates, whose principal values of $[\varepsilon]$ and $[\mu]$ are assumed to be $(\varepsilon_{x1} = 9.4, \varepsilon_{y1} = 11.6, \varepsilon_{z1} = 9.4)$ and $(\mu_{x2} = 1.46, \mu_{y2} = 1.32, \mu_{z2} = 1.25)$, respectively. First, the frequency response of this transmission line is presented, when the principal axes of both tensors are assumed to be misaligned with those of the structure. Notice from Fig. 3 that there is hardly any change in the propagation characteristics from 5 to 50 GHz. The effects of misalignment, namely as $(\theta, \Delta\theta)$ are changed, are confined

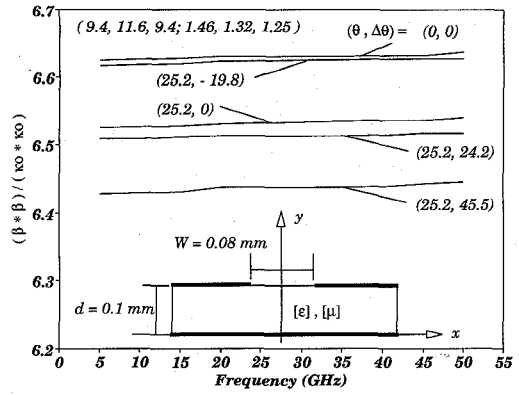

Fig. 3. Frequency dependence of $(n_{\text{eff}})^2$ for an open conductor-backed slotline (odd mode) with $(\theta, \Delta\theta) = (0.0°, 0.0°)$, $(25.2°, -19.8°)$, $(25.2°, 0.0°)$, $(25.2°, 24.2°)$, and $(25.2°, 45.5°)$.

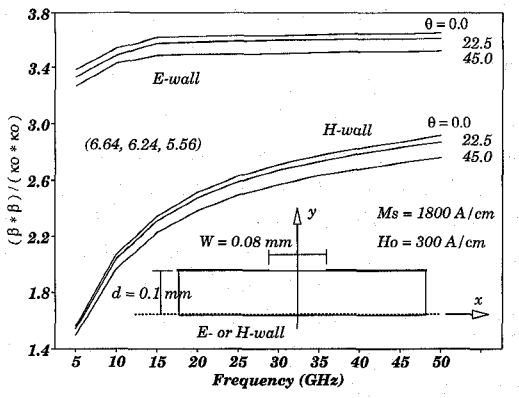

Fig. 5. Frequency dependence of $(n_{\text{eff}})^2$ for E- and H-wall symmetries of an open bilateral slotline with $\theta = 0.0°, 22.5°, 45.0°$, and $M_s = 1800$ A/cm, $H_0 = 300$ A/cm.

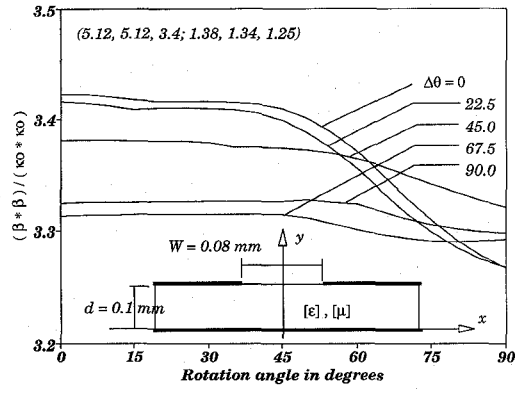

Fig. 4. $(n_{\text{eff}})^2$ as a function of the rotation angle with $\Delta\theta = 0.0°, 22.5°, 45.0°, 67.5°$ and $90.0°$ at $f = 40$ GHz for an open conductor-backed slotline.

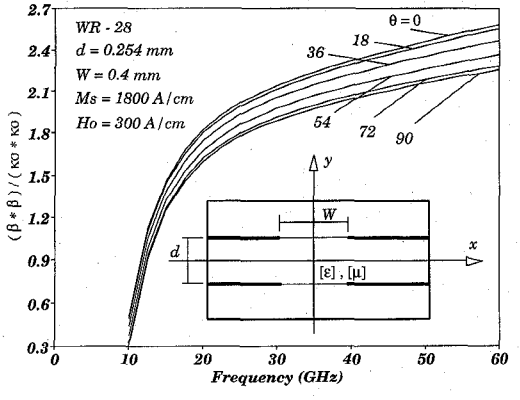

Fig. 6. Frequency dependence of $(n_{\text{eff}})^2$ for a shielded bilateral slotline with $\theta = 0.0°, 18.0°, 36.0°, 54.0°, 72.0°$, and $90.0°$, $(\varepsilon_{x1} = 6.64, \varepsilon_{y1} = 6.24, \varepsilon_{z1} = 5.56)$, and $M_s = 1800$ A/cm, $H_0 = 300$ A/cm.

to lowering the values of $(n_{\text{eff}})^2 = (\beta/k_0)^2$ only. On the other hand, when frequency is fixed at 40 GHz, and the angle θ varies from 0° to 90° for prescribed values of $\Delta\theta$, the slotline for the most part still retains its nondispersive nature. Although, when $\Delta\theta$ is 0° or 22.5°, there is a noticeable change in $(n_{\text{eff}})^2 = (\beta/k_0)^2$ as θ becomes 45°.

Now, numerical results for an open bilateral slotline are presented. In addition to the electric conductor-backed mode (odd symmetry), the even symmetry (magnetic conductor-backed) case is also considered. This time, the substrate is partially characterized by dielectrically anisotropic permittivity $(\varepsilon_{x1} = 6.64, \varepsilon_{y1} = 6.24, \varepsilon_{z1} = 5.56)$. For generality, it is also assumed to be permeable, when exposed to magnetic dc fields. Its magnetic properties will be simulated by a Hermitian permeability tensor, provided that $M_s = 1800$ A/cm and $H_0 = 300$ A/cm.

Fig. 5 contains dispersion curves for both odd and even modes; in other words, electric and magnetic wall symmetries. Rotation effects for the permittivity tensor $(\varepsilon_{x1} = 6.64, \varepsilon_{y1} = 6.24, \varepsilon_{z1} = 5.56)$ that is also anisotropic in $[\mu]$ are included as well, showing that $(n_{\text{eff}})^2 = (\beta/k_0)^2$ can be lowered by increasing the misalignment angle. Computed data also indicate that the even mode is much more sensitive to variation in the frequency than is the odd mode of this structure.

Finally, the propagation characteristics were calculated for the shielded bilateral slotline (finline) having the same medium parameters as the open slotline discussed above. Results for the dominant (H-wall) mode displaying the frequency dependence are shown in Fig. 6. It is clear that the effects of the rotation are most profound at higher frequencies, rather than close to cutoff. Comparison of these results to those corresponding to the H-wall mode of an open bilateral slotline points to some similarities. Specifically, in both cases, the increasing value of θ reduces the magnitude of $(n_{\text{eff}})^2 = (\beta/k_0)^2$, particularly at higher frequencies. In addition, the even mode for both the shielded and open structure is seen to be highly dispersive over the entire range of the selected frequency band.

All computations for the validation and other data, appearing in this paper, were carried out on an IBM compatible 33 MHz, 486-based PC. It was found that four and seven expansion functions were required to achieve convergence for shielded and open transmission lines, respectively. In addition, for shielded lines 250 Fourier (spectral) terms were used to account for x-dependence of the fields. Typical CPU times

were 18 and 60 seconds for shielded and open slotlines, respectively.

IV. Conclusion

Dispersion characteristics of open and shielded bilateral slotlines printed on anisotropic substrate materials were examined in this paper. The formulation was based on differential matrix operators and the spectral-domain method. The admittance Green's functions for open and fully enclosed structures were obtained for substrates that can be of the gyroelectric-type, a Ferrite, or both. Numerous results for the propagation constants of these structures were presented as functions of the frequency as well as the rotation angle of the principal axes of the material.

Appendix

Linear differential operators of (5) are defined as:

$$a_{11} = \mu_{xx}\frac{d^2}{dy^2} + \left(k_0^2\varepsilon_{xx} - \frac{\beta^2}{\mu_{yy}}\right)\mu_d \tag{A1}$$

$$a_{12} = j(\beta\mu_{zx} + \alpha\mu_{xz})\frac{d}{dy} \tag{A2}$$

$$a_{13} = \mu_{zx}\frac{d^2}{dy^2} + \left(\frac{\alpha\beta}{\mu_{yy}} + k_0^2\varepsilon_{xz}\right)\mu_d \tag{A3}$$

$$a_{21} = \frac{j(\alpha\mu_{xx} + \beta\mu_{xz})}{G_0}\frac{d}{dy} \tag{A4}$$

$$a_{22} = -1 \tag{A5}$$

$$a_{23} = \frac{j(\alpha\mu_{zx} + \beta\mu_{zz})}{G_0}\frac{d}{dy} \tag{A6}$$

$$a_{31} = \mu_{xz}\frac{d^2}{dy^2} + \left(k_0^2\varepsilon_{zx} + \frac{\alpha\beta}{\mu_{yy}}\right)\mu_d \tag{A7}$$

$$a_{32} = j(\alpha\mu_{xz} + \beta\mu_{zz})\frac{d}{dy} \tag{A8}$$

$$a_{33} = \mu_{zz}\frac{d^2}{dy^2} + \left(k_0^2\varepsilon_{zz} - \frac{\alpha^2}{\mu_{yy}}\right)\mu_d \tag{A9}$$

where $\mu_d = \mu_{xx}\mu_{zz} - \mu_{xz}\mu_{zx}$, and

$$G_0 = \alpha^2\mu_{xx} + \beta^2\mu_{zz} + \alpha\beta(\mu_{xz} + \mu_{zx}) - k_0^2\varepsilon_{yy}\mu_d\,. \tag{A10}$$

In the aforementioned equations, β is the propagation constant along the z-direction, α is the Fourier transform variable, and k_o is the propagation constant of free-space.

The coefficients of the coupled, second-order differential matrix (6) for $\tilde{E}_x$ and $\tilde{E}_z$ are listed below:

$$a_0 = \left(k_0^2\varepsilon_{xx} - \frac{\beta^2}{\mu_{yy}}\right)\mu_d G_0 \tag{A11}$$

$$a_2 = \beta^2\mu_d - k_0^2\varepsilon_{yy}\mu_{xx}\mu_d \tag{A12}$$

$$b_0 = \left(k_0^2\varepsilon_{xz} + \frac{\alpha\beta}{\mu_{yy}}\right)\mu_d G_0 \tag{A13}$$

$$b_2 = -\alpha\beta\mu_d - k_0^2\varepsilon_{yy}\mu_{zx}\mu_d \tag{A14}$$

$$c_0 = \left(k_0^2\varepsilon_{zx} + \frac{\alpha\beta}{\mu_{yy}}\right)\mu_d G_0 \tag{A15}$$

$$c_2 = -\alpha\beta\mu_d - k_0^2\varepsilon_{yy}\mu_{xz}\mu_d \tag{A16}$$

$$d_0 = \left(k_0^2\varepsilon_{zz} - \frac{\alpha^2}{\mu_{yy}}\right)\mu_d G_0 \tag{A17}$$

$$d_2 = \alpha^2\mu_d - k_0^2\varepsilon_{yy}\mu_{zz}\mu_d\,. \tag{A18}$$

Finally, the expressions for the elements of the admittance Green's function defined in (9) are given by

$$\tilde{Y}_{zz}(\alpha,\beta) = \frac{\delta_2' q_{11} - \delta_1' q_{12}}{\delta_2' - \delta_1'} \tag{A19}$$

$$\tilde{Y}_{zx}(\alpha,\beta) = \frac{q_{11} - q_{12}}{\delta_2' - \delta_1'} \tag{A20}$$

$$\tilde{Y}_{xz}(\alpha,\beta) = \frac{\delta_1' q_{22} - \delta_2' q_{21}}{\delta_2' - \delta_1'} \tag{A21}$$

$$\tilde{Y}_{xx}(\alpha,\beta) = \frac{q_{22} - q_{21}}{\delta_2' - \delta_1'} \tag{A22}$$

with

$$\delta_1' = \frac{b_2\gamma_a^2 + b_0}{a_2\gamma_a^2 + a_0} \tag{A23}$$

$$\delta_2' = \frac{b_2\gamma_b^2 + b_0}{a_2\gamma_b^2 + a_0} \tag{A24}$$

$$q_{11} = \frac{\gamma_a}{z_t}(c_2\delta_1' - d_2)\begin{Bmatrix} th_a^m \\ ct_a^e \end{Bmatrix} - \frac{\beta(\beta - \alpha\delta_1')}{\gamma_{y1}(\alpha^2+\beta^2)} \cdot \begin{Bmatrix} f^o \\ f^s \end{Bmatrix} - \frac{\alpha\gamma_{z1}(\alpha + \beta\delta_1')}{(\alpha^2+\beta^2)}\begin{Bmatrix} f^o \\ f^s \end{Bmatrix} \tag{A25}$$

$$q_{12} = \frac{\gamma_b}{z_t}(c_2\delta_2' - d_2)\begin{Bmatrix} th_b^m \\ ct_b^e \end{Bmatrix} - \frac{\beta(\beta - \alpha\delta_2')}{\gamma_{y1}(\alpha^2+\beta^2)} \cdot \begin{Bmatrix} f^o \\ f^s \end{Bmatrix} - \frac{\alpha\gamma_{z1}(\alpha + \beta\delta_2')}{(\alpha^2+\beta^2)}\begin{Bmatrix} f^o \\ f^s \end{Bmatrix} \tag{A26}$$

$$q_{21} = \frac{\gamma_a}{z_t}(b_2 - a_2\delta_1')\begin{Bmatrix} th_a^m \\ ct_a^e \end{Bmatrix} + \frac{\alpha(\beta - \alpha\delta_1')}{\gamma_{y1}(\alpha^2+\beta^2)} \cdot \begin{Bmatrix} f^o \\ f^s \end{Bmatrix} - \frac{\beta\gamma_{z1}(\alpha + \beta\delta_1')}{(\alpha^2+\beta^2)}\begin{Bmatrix} f^o \\ f^s \end{Bmatrix} \tag{A27}$$

$$q_{22} = \frac{\gamma_b}{z_t}(b_2 - a_2\delta_2')\begin{Bmatrix} th_b^m \\ ct_b^e \end{Bmatrix} + \frac{\alpha(\beta - \alpha\delta_2')}{\gamma_{y1}(\alpha^2+\beta^2)} \cdot \begin{Bmatrix} f^o \\ f^s \end{Bmatrix} - \frac{\beta\gamma_{z1}(\alpha + \beta\delta_2')}{(\alpha^2+\beta^2)}\begin{Bmatrix} f^o \\ f^s \end{Bmatrix}, \tag{A28}$$

where $th_{a,b}^m$ and $ct_{a,b}^e$ are multiplying factors for the magnetic or electrical walls, and $f^{o,s}$ corresponds to open or shielded structures, respectively. Their explicit forms are given by

$$th_{a,b}^m = \tan h\left(\gamma_{a,b}\frac{d}{2}\right) \tag{A29}$$

$$ct_{a,b}^e = \cot h\left(\gamma_{a,b}\frac{d}{2}\right) \tag{A30}$$

$$f^o = 1 \tag{A31}$$

$$f^s = \cot h\gamma_1\left(b - \frac{d}{2}\right), \tag{A32}$$

and the remaining parameters appearing above are

$$\gamma_1 = \sqrt{\alpha^2 + \beta^2 - k_0^2} \tag{A33}$$

$$z_t = j\omega\mu_0\mu_d G_0 \tag{A34}$$

$$\gamma_{y1} = \frac{\gamma_1}{j\omega\varepsilon_0} \tag{A35}$$

$$\gamma_{z1} = \frac{\gamma_1}{j\omega\mu_0}, \tag{A36}$$

where γ_1 is the transverse propagation constant of the air region.

REFERENCES

[1] P. J. Meier, "Integrated fin-line millimeter components," *IEEE Trans. Microwave Theory Tech.*, vol. MTT-22, no. 12, pp. 1209–1216, Dec. 1974.

[2] K. C. Gupta, R. Garg, and I. J. Bahl, *Microstrip Lines and Slotlines.* Dedham, MA: Artech, 1979, chs. 5 and 6.

[3] K. S. Yngvensson, T. L. Korzeniowski, Y.-S. Kim, E. L. Kollberg and J. F. Johansson, "The tapered slot antenna—A new integrated element for millimeter-wave applications," *IEEE Trans. Microwave Theory Tech.*, vol. MTT-37, no. 2, pp. 365–374, Feb. 1989.

[4] R. Janaswamy, "Even-mode characteristics of the bilateral slotline," *IEEE Trans. Microwave Theory Tech.*, vol. MTT-38, no. 6, pp. 760–765, June 1990.

[5] H. Shigesawa, M. Tsuji, and A. A. Oliner, "Conductor-backed slotline and coplanar waveguide: Dangers and full-wave analyses," in *IEEE MTT-S Int. Microwave Symp. Dig.*, June 1988, pp. 199–202.

[6] J. Bormemann, "A scattering-type transverse resonance formulation and its application to open, conductor-backed and shielded (M)MIC slotline structures," in *IEEE MTT-S Int. Microwave Symp. Dig.*, June 1991, pp. 695–698.

[7] H. Yang and N. Alexopoulos, "Uniaxial and biaxial substrate effects on finline characteristics," *IEEE Trans. Microwave Theory Tech.*, vol. MTT-35, no. 1, pp. 24–29, Jan. 1987.

[8] F. Medina, M. Horno, and H. Baudrand, "Generalized spectral analysis of planar lines on layered media including uniaxial and biaxial dielectric substrates," *IEEE Trans. Microwave Theory Tech.*, vol. MTT-37, no. 3, pp. 504–511, Mar. 1989.

[9] T. Q. Ho and B. Beker, "Effects of misalignment on propagation characteristics of transmission lines printed on anisoptropic substrates," *IEEE Trans. Microwave Theory Tech.*, vol. MTT-40, no. 5, pp. 1018–1021, May 1992.

[10] M. Geshiro, S. Yagi, and S. Sawa, "Analysis of slotlines and microstrip lines on anisotropic substrates," *IEEE Trans. Microwave Theory Tech.*, vol. MTT-39, no. 1, pp. 64–69, Jan. 1991.

[11] T. Kitazawa and T. Itoh, "Asymmetrical coplanar waveguide with finite metallization thickness containing anisotropic media," *IEEE Trans. Microwave Theory Tech.*, vol. MTT-39, no. 8, pp. 1426–1433, Aug. 1991.

[12] Y. Chen and B. Beker, "Analysis of single and coupled microstrip lines on anisotropic substrates using differential matrix operators and the spectral-domain method," *IEEE Trans. Microwave Theory Tech.*, vol. MTT-41, no. 1, pp. 123–128 Jan. 1993.

[13] T. Itoh (ed.), *Numerical Techniques for Microwave and Millimeter-wave Passive Structures.* New York: Wiley, 1989.

[14] R. E. Collin, *Foundations for Microwave Engineering.* New York: McGraw-Hill, 1966, ch. 6, Sect. 6.6.

Yinchao Chen received the B.S. degree in physics from the National Wuhan University, China, the M.S.E.E. degree from the University of Science and Technology of China, and Nanjing Research Institute of Electronics Technology, and the Ph.D. degree from the University of South Carolina in electrical engineering, in 1982, 1985, and 1992, respectively.

From 1982 to 1988, he was with the Microwave and Antenna Laboratory, Nanjing Research Institute of Electronics Technology, as an engineer and research group leader working with design, research, and synthesis of microwave components and antennas. From 1988 to 1989, he was a Research Assistant, in the Department of Physics, University of Tennessee, Knoxville, TN, and since 1989, he has been with the Department of Electrical and Computer Engineering, University of South Carolina, Columbia, SC, as a Research and Teaching Assistant. Currently, he is a Postdoctoral Fellow in the Department, working with theory and analysis of MICs and their discontinuities.

His academic interests include microwave and millimeter-wave integrated circuits, radiation, scattering, and propagation theories and applications.

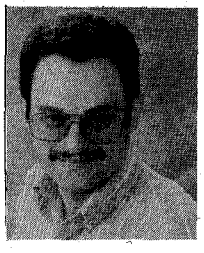

Benjamin Beker (S'83–M'88) was born in Vilnius, Lithuania, in 1959. He received the B.S.E.E., M.S.E.E., and the Ph.D. degrees from the University of Illinois, Chicago, IL in 1982, 1984, and 1988, respectively.

From 1982 to 1988 he was a Research Assistant in the Department of Electrical Engineering and Computer Science at the University of Illinois, Chicago, working with numerically oriented scattering and radiation problems. In 1988, he joined the Department of Electrical and Computer Engineering at the University of South Carolina, Columbia, where he now is Associate Professor.

His research interests include EM field interaction with anisotropic materials, computational methods in scattering, radiation, and guided-wave propagation in millimeter-wave integrated circuits, and electronic packaging.